World Applied Sciences Journal 12 (4): 446-459, 2011
ISSN 1818-4952

Application of a Coupling Algorithm for the Simulation of Flow and Pollution in Open Channels

A. Mahjoob and R. Ghiassi

Department of Civil Engineering, Tehran University, Tehran, Iran

Abstract: A hybrid numerical scheme has been presented in this paper for channel flow simulation by coupling one-dimensional and two-dimensional models. Both 1D and 2D differential equations have been discretized by applying the finite volume cell-centered method in a collocated grid system and solved along channel axis for all sections and elements. Due to truncation, dissipation and round off errors, using numerical methods for domains with great number of elements that require huge computations may lead to some sort of divergence. This problem is highlighted, when a collocated grid system is dealt with. To reduce divergence and instability, 2D results of water level and cross section discharge have been compared with those of the 1D results where needed and adjusted properly. Double simulation provides some other advantages as described in the paper. In order to simulate a 2D flow in a channel network, a new sequential implicit scheme has been also suggested and applied. In addition to the above, 2D advection-diffusion equation has been discretized based on general finite volume method to simulate pollution. Three test cases are discussed for proving the mentioned techniques: (a) 2D flow modeling in a meandering channel with 90° bends by applying 1D-2D hybrid model, (b) 2D flow simulation at a 90° open-channel junction by applying both 1D-2D hybrid model and sequential implicit scheme at the junction and (c) tracer test in the *S*-curved Channel. The comparisons show the advantages of the proposed hybrid scheme for 2D flow and pollution simulation. Also the results show the ability and accuracy of sequential implicit scheme for channel network simulation.

Key words: Hybrid 1D-2D model · Sequential implicit scheme · Channel network · Pollution model · Curved channel · Finite Volume.

INTRODUCTION

During the past two decades, free surface flow numerical modeling has developed rapidly and today it is very popular among scientists and engineers for environmental applications and optimum design of river structures [1]. In most rivers and channels, two-dimensional (2D) depth-averaged equations can be used by integrating the three- dimensional (3D) governing equations over the flow depth [2-4]. Also, since the channel flow may be assumed one-dimensional (1D), the 1D governing equations may be obtained from integrating the 3D governing equations over the flow area as reported in the literature [5-8].

Finite Difference Methods [9-11], Finite Element Methods [12] and Finite Volume Methods (FVM) [10,13,14] are commonly used methods that have been applied to solve 2D governing equations. Finite volume methods have several advantages over finite difference and finite element approaches, addressed in the literature. Flexibility, for complex geometric domain descretization in comparison with the finite difference and simplicity of equation discretization, in comparison with the finite element, can be mentioned as the main advantages. The integral form of the conservation equations are used in the finite volume methods [15,16]. Hence, the mass and momentum remain conserved [17].

1D flow models provide average flow velocity and water elevation in each channel cross section. 2D hydrodynamic models in plan provide horizontal velocity components and water height in each element. These models can predict water eddies behind spur dikes, bridge piers, river expansion and water intakes. Hence, for local sedimentation and scour modeling in the mentioned locations, 2D models need to be developed. Also, for environmental simulations, 2D models provide more details of parameter variation within the computational domain. However, 2D modeling is more

Corresponding Author: A. Mahjoob, Department of Civil Engineering, Tehran University, Tehran, Iran.
E-mail: amahjoob@ut.ac.ir.

complex than 1D simulation and since 2D models need more information and a higher proficiency level, they impose more time and cost.

From computational point of view, 2D simulation complexity is mainly due to the increase in the number of elements and equations per element that result in heavy computations and consequently, increasing errors.

2D modeling of channel flow involves a huge number of computations, especially where the domain discretization is a boundary fitted type (or curvilinear) to simulate the natural domain as best as possible. Due to truncation errors of equation discretizations, dissipation and round off errors, more computation leads to more unexpected errors which may cause some instability and oscillation problems. In some modeling such as shock capturing phenomena (e.g. flood modeling in rivers), it is important to reduce the effect of numerical truncation and dissipation errors and many researchers have tried to overcome this problem using some especial schemes.

Alcrudo and Garcia Navarro used the McCormack scheme, corrected by the Total Variation Diminishing (TVD), to reduce spurious oscillations around discontinuities, both for 1D and 2D flow problems [18]. Delis *et al.* developed three implicit high-resolution TVD schemes to solve Saint Venant equations and in investigated the applicability, performance and validity of these methods [19]. Macchione and Assunta developed a finite-volume numerical method for solving the unsteady, three-dimensional Reynolds-averaged Navier-Stokes equations in generalized curvilinear coordinates. They compared the TVD, upwind and central schemes while they were used to capture shocks for dam break problems [20]. Mambretti *et al.* used artificial additional terms in the original form of the McCormack scheme to avoid spurious oscillations and discontinuities without any physical significance [21]. Zhao *et al.* introduced three different first-order upwind schemes, including the Osher, the Roe and the SWS schemes, into 2D shallow water equations. These schemes, that can capture the shock waves without oscillations, were successfully implemented in the FVM [22]. Zarrati and Jin applied staggered grid to avoid the so-called checkerboard non-physical pressure oscillations and excessive interpolations [23]. Aliparast developed a numerical model based upon a second-order upwind cell-centered finite volume method on unstructured triangular grids for solving shallow water equations. He also handled discontinuous solutions using Harten-Lax-vau Leer (HLL) approximate Riemann solver [24].

Also, Long rivers pass several ranges of path types from narrow valleys to wide flat plains. Some researchers consider a bound of a river where it comes out from the mountains and enters the plain. They link a 1D river model in the mountain domain with a 2D shallow water model in the plain area. 1D equations are solved in the upstream part and 2D equations are solved in the down stream area and some especial links are considered in their joint.

Miglio *et al.* presented a model coupling technique to reduce computational cost in a complex hydrodynamic configuration by suitably coupling one and 2D models. He explained his technique as a dimensionally heterogeneous and physically homogeneous coupling strategy that is driven by a priori physical considerations. Some assumptions have been considered at the interface of 1D and 2D domains [25]. Fang-li *et al.* coupled 1D and 2D models to simulate the dam break flow in river courses and downstream areas at the same time while the water level was higher than the elevation of levee there [26]. Gejadze and Monnier coupled 1D shallow water equations with storage areas (global model) and 2D shallow water equations (zoom model) using the optimal control approach. The zoom model is used to assimilate local observations into the global model (variational data assimilation) by playing the part of a mapping operator [27].

On the other hand, in some low-slope regions like plains, rivers may be branching; or in alluvial plains where the slop is low, meanders may appear. Therefore, it is important to learn the behaviour of rivers in branching location and to simulate water flow in branching part of rivers [28]. For implicit (or semi implicit) flow simulation in channel network, whole geometry domain (including all branches) is discretized and the governing equations are solved simultaneously. In such scheme, dimension of coefficients matrix and consequently computational costs, are directly proportional to the number of elements. Numerical and laboratory modeling of flow in branched channels with symmetrical geometry and varying hydraulic conditions are investigated by Yousefi *et al.* [29]. They applied ADI scheme for solving the discretized equations in whole domain and compared numerical results against experimental data. Neary *et al.* [30] developed a finite difference hydrodynamic model to simulate channel junction flow. Implicit method was used to solve discretized pressure equation in whole domain. Huang *et al.* developed a numerical model to investigate the open-channel junction flow. The pressure implicit splitting of operator algorithm was adopted and equations

of whole geometry domain were solved simultaneously. The model was applied to investigate the effect of the junction angle on the flow characteristics and a discussion of the results was presented [31].

In this paper, another coupling algorithm for construction of a hybrid 2D and 1D channel flow model is presented. In this proposed technique, 1D channel flow data is applied to adjust 2D free surface flow parameters. The discretization of both sets of equations (1D and 2D) is obtained by the finite volume cell centered type method. 1D and 2D equations are discretized and solved simultaneously along longitudinal river axis for all sections and elements. To reduce 2D result oscillations and any kind of divergence, instability and numerical error problems, water depth and flow discharge are adjusted by using 1D results where needed. Also, in order to simulate a channel network, a new sequential technique has been suggested that can increase computational speed and reduce its cost. It has been explained in section 3.3.

Results of the 2D hydrodynamic model are then applied in an environmental model to simulate pollution transportation. The environmental model solves depth-averaged advection-dispersion equations to predict pollution distribution in the channel. This model is also developed based on finite volume discretization of the governing equation in a boundary fitted curvilinear coordinate mesh system.

The hydrodynamic model is verified for two test cases of open channel flow including flow in a meandering channel with 90° bends [32] and Flow at a 90° open-channel junction [33]. The environmental model is applied for a tracer test in the S-curved channel [34]. The results of the tests demonstrate the ability and accuracy of the coupling algorithm to simulate the 2D free surface flow in a channel media type and its results are valid for pollution distribution simulation.

Governing Equations: The governing differential equations for both 1D and 2D simulations are as follows:

Two Dimensional Governing Equations: By assuming the pressure distribution to be hydrostatic and neglecting both wind shear stress and Coriolis acceleration, the following 2D depth-averaged flow equations are obtained by integrating the 3D Navier-Stokes equations over the flow depth [4, 29]:

$$\frac{\partial \zeta}{\partial t}+\frac{\partial (UH)}{\partial x}+\frac{\partial (VH)}{\partial y}=0 \tag{1}$$

$$\frac{\partial (UH)}{\partial t}+\frac{\partial (U^2H)}{\partial x}+\frac{\partial (UVH)}{\partial y}= -gH\frac{\partial (\zeta)}{\partial x}+\frac{\partial (H\tau_{xx})}{\partial x}+\frac{\partial (H\tau_{xy})}{\partial y}-\tau_{xz}\big|_{-H} \tag{2}$$

$$\frac{\partial (VH)}{\partial t}+\frac{\partial (UVH)}{\partial x}+\frac{\partial (V^2H)}{\partial y}= -gH\frac{\partial (\zeta)}{\partial y}+\frac{\partial (H\tau_{yx})}{\partial x}+\frac{\partial (H\tau_{yy})}{\partial y}-\tau_{yz}\big|_{-H} \tag{3}$$

Where ξ = water surface elevation, H = flow depth, g = gravitational acceleration, U and V = depth-averaged velocities in the x and y directions respectively in the forms:

$$U=\frac{1}{H}\int_{z_b}^{H+z_b} u\,dz \qquad V=\frac{1}{H}\int_{z_b}^{H+z_b} v\,dz \tag{4}$$

and z_b = elevation of channel bed. The bottom shear stresses are estimated according to the following formulas:

$$\tau_{xz}\big|_{-H}=\frac{g}{H^{\frac{1}{3}}}n^2U\sqrt{U^2+V^2} \tag{5}$$

$$\tau_{yz}\big|_{-H}=\frac{g}{H^{\frac{1}{3}}}n^2V\sqrt{U^2+V^2} \tag{6}$$

Where n = the Manning coefficient. τ_{xy}, τ_{yy}, τ_{yx} and τ_{yx} are the depth-averaged internal shear stresses that are defined as follows:

$$\tau_{xx}=(\upsilon_l+\upsilon_t)\frac{\partial U}{\partial x} \quad \tau_{xy}=(\upsilon_l+\upsilon_t)\frac{\partial U}{\partial y} \tag{7}$$

$$\tau_{yx}=(\upsilon_l+\upsilon_t)\frac{\partial V}{\partial x} \quad \tau_{yy}=(\upsilon_l+\upsilon_t)\frac{\partial V}{\partial y} \tag{8}$$

Where $\upsilon_l=1.14\times10^{-6}m^2s^{-1}$ laminar kinematic viscosity and υ_t = the kinematic eddy viscosity and can be estimated from $\nu_t=0.15nH^{0.83}\sqrt{g(U^2+V^2)}$ [34].

The 2D depth-averaged form of the advection-dispersion equation can be written as follows [34]:

$$\frac{\partial (CH)}{\partial t}+\frac{\partial (HUC)}{\partial x}+\frac{\partial (HVC)}{\partial y}= \frac{\partial}{\partial x}\left(HD_L\frac{\partial C}{\partial x}\right)+\frac{\partial}{\partial y}\left(HD_T\frac{\partial C}{\partial y}\right)+C_0 \tag{9}$$

Where C = the depth-averaged concentration, D_L = longitudinal dispersion coefficient, D_T = transverse dispersion coefficient and C_o = source or sink terms that can be given as initial or boundary conditions.

Governing Equations of One Dimensional Model: For the development of the 1D model, some simplifications were assumed [33]. The water is incompressible and homogeneous. The vertical pressure distribution of flow is hydrostatic. Hence, the flow can be described by the Saint Venant equations [7]:

$$\frac{\partial A}{\partial t}+\frac{\partial Q}{\partial x}=q_l \tag{10}$$

$$\frac{\partial Q}{\partial t}+\frac{\partial}{\partial x}\left(\frac{\beta Q^2}{A}\right)+gA\frac{\partial \zeta}{\partial x}+gA(S_f-S_0)=V_{lp}q_l \tag{11}$$

Where x= longitudinal distance along the channel, t= time, A= area cross section, Q= flow discharge, ξ = water surface level, S_0 = channel bottom slope, g = gravity acceleration, S_f= slope of energy grade line ($S_f=\frac{n^2\tilde{u}|\tilde{u}|}{R^{4/3}}$, $\tilde{u}$ = mean flow velocity ($\tilde{u}=Q/A$), n= the Manning roughness factor as used in Eq. (5) Eq. and (6)), β = the correction factor for momentum due to the nonuniform velocity distribution over the cross section [$\beta=\frac{1}{\tilde{u}^2A}\int_A u_l^2 dA$ where u_l = Longitudinal component of velocity and for each element, it can be calculated from U, V (two dimensional analysis results) and direction of element as shown in Fig. 1 ($u_l=U\cos\theta+V\sin\theta$)], q_l= lateral discharge in unit length and V_{lp}= lateral flow velocity component parallel to t he main channel direction .

Discretization and Solution Scheme: The governing equations are discretized using the finite volume approach. The process is as follows:

Two Dimensional Equation Discretization: The computational domain for 2D modeling is discretized by applying a boundary fitted mesh into a set of quadrilateral cells as shown in Fig. 2. 2D governing equations presented in 2.1 are discretized by using the finite volume method. The flow parameters are computed based on cell centered assumptions. Cell edges are defined as the faces of a quadrilateral element.

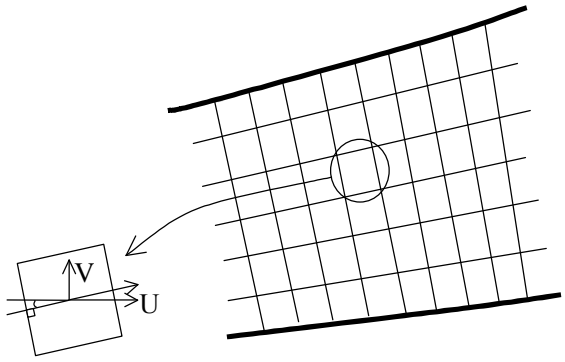

Fig. 1: Longitudinal component of velocity in a 2D element

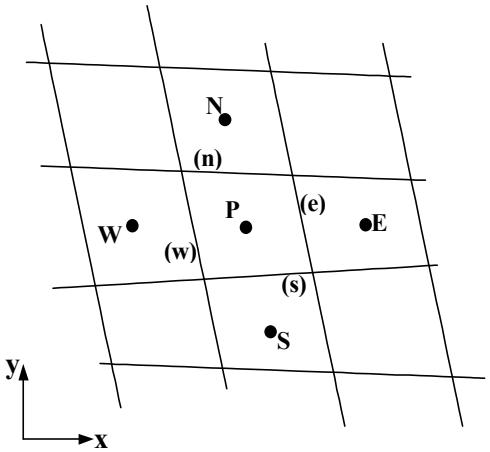

Fig. 2: Two dimensional cell centered volume

Depth-averaged continuity, momentum and advection-dispersion equations can be rewritten as the following general format:

$$\frac{\partial M}{\partial t}+\nabla B=C \tag{12}$$

By integrating Eq. (12) over the quadrilateral element $\dot{U}_i$, we will have:

$$\int_{\Omega_i}\left(\frac{\partial M}{\partial t}+\nabla B\right)d\Omega=\int_{\Omega_i}C\,d\Omega \tag{13}$$

By assuming M_i to be the average value of parameter M within the cell $\dot{U}_i$ (considered at the cell centre), the above equation becomes:

$$\frac{\partial M_i}{\partial t}A_i+\oint_L B.n\,ds=C\,A_i \tag{14}$$

Where A_i = cell surface area and L= boundary of the cell surface (both in the xy plane). Considering that the surface integral is approximated by summation of the flux

vector over each edge of the quadrilateral cell, the second term of Eq. (14) can be rewritten as follows:

$$\oint_L B.n\,ds = \sum_{j=1}^{4} B_{ij}\,\Delta l_{ij} \tag{15}$$

Where l_{ij}= the jth edge of cell, Ω_i ,Δl_{ij}= the length of l_{ij}, B_{ij}= the numerical flux through the edge l_{ij}.

The Alternating Direction Implicit (ADI) scheme [30,9] and Thomas algorithm for Tri-Diagonal Matrix Analysis (TDMA) [32] were then applied to solve the discretized algebraic equations.

Since numerical errors and instability are fairly low in 1D results, they can be used to moderate 2D results. In this paper, to adjust 2D computational results against 1D data, the following steps are carried out.

- Discharge Adjustment. In the proposed hybrid scheme, it is assumed that there must be no difference between the discharge value at section i from 2D model and that of the 1D model. The difference between the mentioned discharges can be defined as:

$$q_i = \left| (\sum_{j=1}^{j_{y\max}} Q_{i,j_{2D}}) - (Q_{i_{1D}}) \right| \tag{16}$$

Where Q_{i1D}= the discharge at section i from 1D model and Q_{i2D} = the discharge at element j of section i from 2D model and $j_{y_{\max}}$ = number of elements on transverse direction at section i. When both 1D and 2D models simulate the nature as it is, the value of q_i tends to zero. Therefore, 2D discharge at section i can be adjusted by the value of 1D discharge.

- Water Surface Elevation Modification. Again, it is assumed that there must be no difference between mean value of water surface elevation at section i computed from both 2D and 1D models. The difference between 2D and 1D water level can be defined by:

$$h_i = \left| (\frac{1}{j_{y_{\max}}} \sum_{j=1}^{j_{y\max}} \zeta_{i,j_{2D}}) - (\zeta_{i_{1D}}) \right| \tag{17}$$

Where $\zeta_{i_{1D}}$ = water surface elevation at section i from 1D model and $\zeta_{i,j_{2D}}$ = water surface elevation at element j of section i from 2D model. If both 1D and 2D models simulate the real nature, the value of h_i tends to zero. So, mean value of water elevation in 2D model at section i can be adjusted by 1D water elevation.

One Dimensional Equation Discretization: For 1D flow modeling, the river is divided into several 1D elements where each element is located between two cross sections, covering all 2D cross river cells, as shown in Fig. 3.

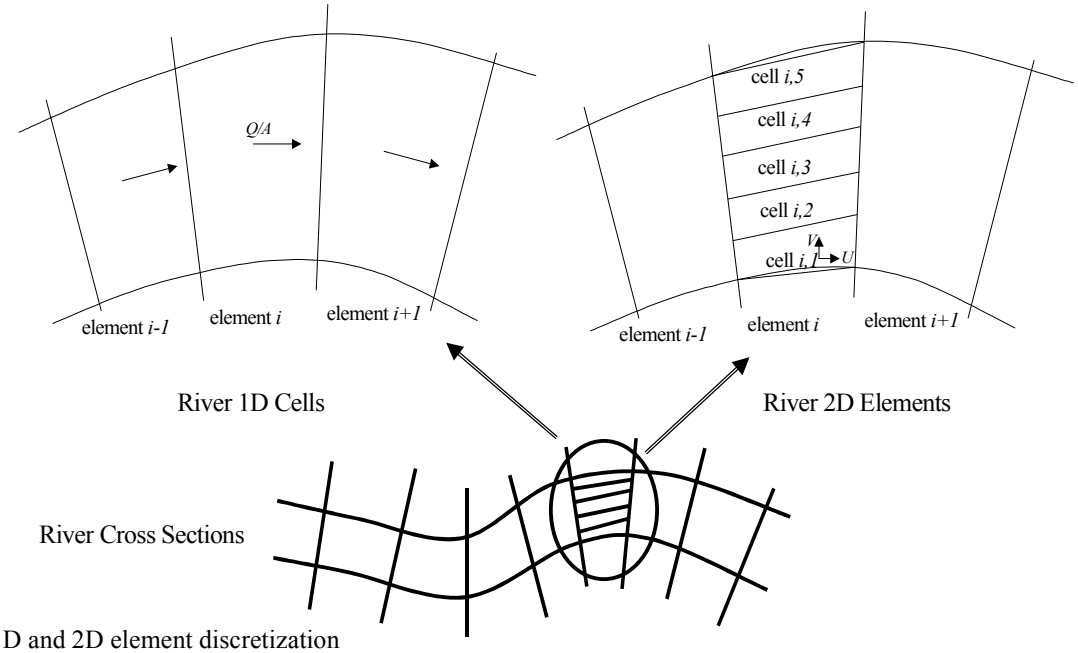

Fig. 3: 1D and 2D element discretization

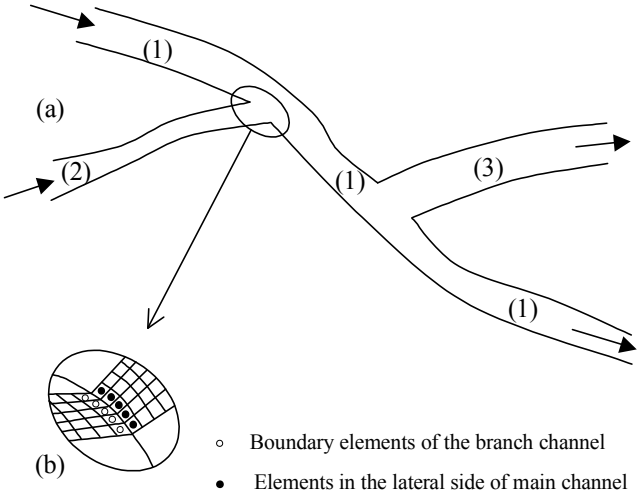

Fig. 4: (a) Schematic view of channel network (b) Plan of junction elements

1D governing equations described in 2.2, are discretized by the finite volume method. The flow parameters are computed based on cell centered assumptions. The equations are solved by the semi implicit scheme. Terms 2 and 4 in the motion Eq. (11) are considered explicitly and the rest of the terms in Eq. (10) and Eq. (11) are considered implicitly. More details of 1D flow modeling may be found at references [5-8].

Channel Network Solution Technique: In this research, a new technique has been presented for 2D flow simulation in channel network. Some researches had been done about sequential 1D channel network modeling [38, 39]. As shown in Fig. 4(a), the main channel is considered as branch number one and the other branches are numbered in order of importance. Each branch is discretized and the respected governing equations are solved separately. In the channel junction, the data of the elements located at the lateral side of the main channel must be linked with the data at the boundary cross section of the branched channel, as shown in Fig. 4(b).

The Solution Scheme Can Be Summarized as the Following Steps:

- All flow data is assumed to be known in the current step: 'n' and must be computed for the next step: 'n+1'
- Flow equations are solved in the main channel by applying upstream and downstream conditions in 'n+1' step and considering flow data at junction lateral elements from the previous solution step 'n' of the branched channel
- Flow equations are solved in each branch by applying given boundary conditions at external boundary and computed flow conditions in the main channel lateral elements in step 'n+1' at the internal boundary. This process is done for all branches based of order of the importance.

This technique is applied for 2D flow simulation of channel network for the first time and can reduce the size of the solution matrix and total number of calculations. Hence, the computational cost is reduced and the convergence rate increased.

Model Verification: To evaluate the performance of the proposed hydrodynamic technique, the model has been applied to three different hydrodynamic test cases: flow in a meandering channel with 90°bends, Flow at a 90° open-channel junction and tracer test in the *S*-curved Channel as described below.

Flow in Meandering Channel with 90° Bends: Laboratory tests were done in an experimental channel consisting of 10 consecutive bends with a rectangular cross section. Each curve was composed of a circular part and a straight reach, so that the centerline of the channel closely followed a sine generated wave [40]. Centerline radius of the bend channel was 0.6 m with 90° angle and length of the straight reach was 0.3 m. Width of the channel was 0.3 m in all the bends and straight parts. For a flow discharge of 0.002 m^3/s and longitudinal bed slope of 1/1000, the average flow depth and Froude number was 0.03 m and 0.42 respectively. Width-to-depth ratio of this channel is therefore equal to 10 with R/B=2.

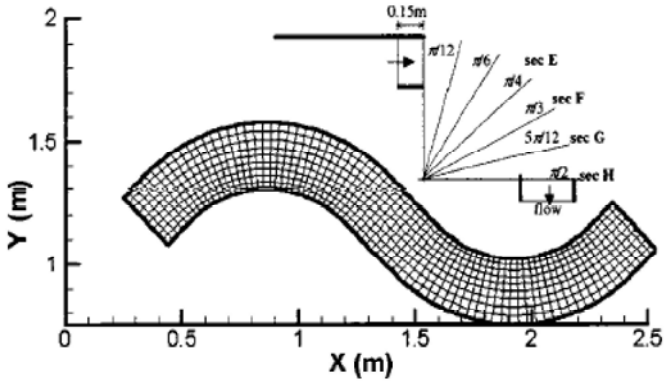

Fig. 5: Layout of the calculated reach and measurement section of the 90° bends

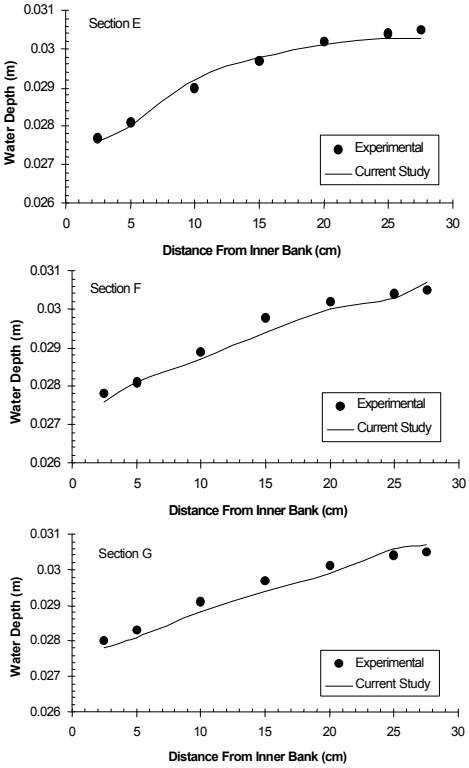

Fig. 6: Comparison of calculated transversal water surface with experimental data of 90° bends

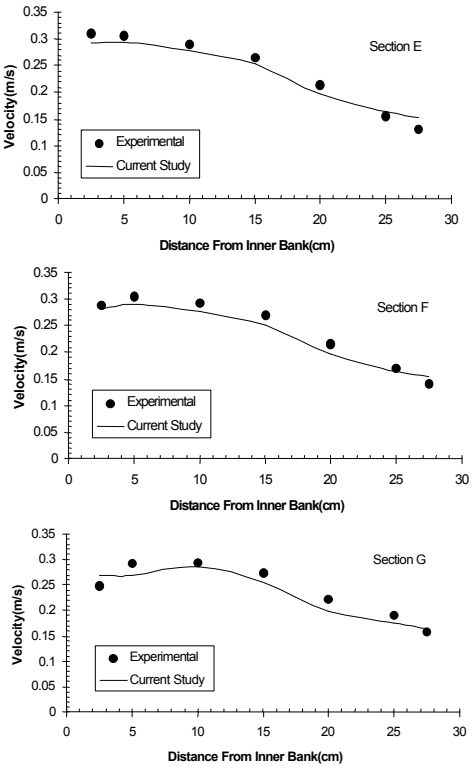

Fig. 7: Comparison of velocity profiles with experimental data of 90° bends

The Manning's roughness coefficient of the channel was about 0.013. The geometry of the experimental channel agrees with the shape of streams encountered in the field and the flow has a moderate Froude number. Transverse water surface profile was measured by static pressure probe and a micro-propeller was utilized for the velocity measurements [40].

An 80 × 10 mesh was generated for two consecutive bends in a form shown in Fig. 5. The downstream section was selected at the straight reach where the water surface was almost constant according to the experimental results. Water surface profiles as well as longitudinal velocity distributions in three sections across a bend (as illustrated in Fig. 5) are compared with the experimental data in Fig. 6 and Fig. 7. The comparison showed that the model predicted the water surface profile and velocity distribution well. Relative water surface elevation error for sections E, F and G located in the channel bend are 0.004, 0.006 and 0.008 respectively. Also relative velocity errors for the same sections are 0.070, 0.061 and 0.068 that shows a very good accuracy of the model.

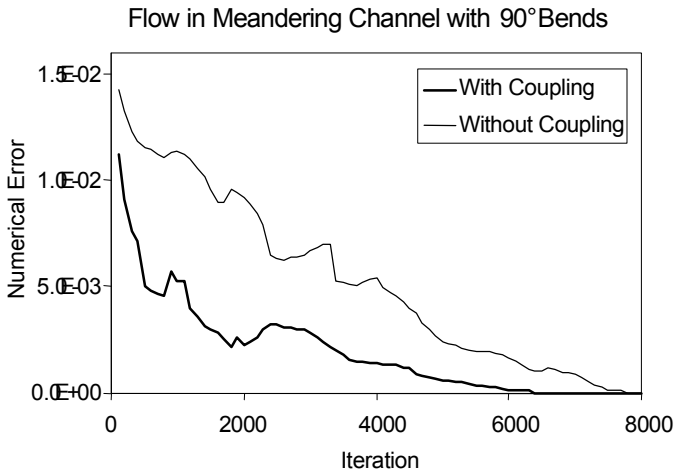

Fig. 8: Numerical error history at flow in meandering channel with 90° bends

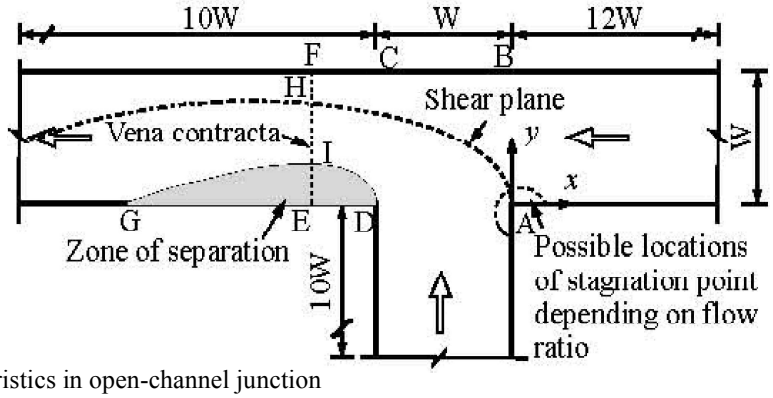

Fig. 9: Flow characteristics in open-channel junction

To show the advantage of the coupling scheme, a convergence test based on the numerical error history was done. As shown in Fig. 8, the model with coupling scheme converges with fewer number of iterations compared with the model without coupling scheme. Coupling scheme is described in section 3.1 and 5.

Flow at a 90° Open-channel Junction: The investigated subject is concerned with the sharp-edged, equal-width 90° junction, reported as an experimental test by Weber [33]. The floor of the entire channel is horizontal and the plane is illustrated in Fig 9. The origin "A" is chosen to be x =0, y =0 and z =0. The coordinate system defined for this simulation has the positive x-axis oriented in the upstream direction of the main channel and the positive z-axis is upward in the vertical direction. The channel consists of a main channel with 21.95 m length and a branch channel with 3.66 m length. The branch channel is located 5.49 m downstream of the entrance of the main channel. Both channels have a width of 0.914 m, designated by W. The total combined flow rate Q_d is 0.17 m^3/s and the downstream depth H_d is held constant at 0.296 m. Therefore, the downstream bulk velocity is V_d = 0.628 m/s, which gives a Froude number of 0.37.

A total of six runs of experiments were conducted. The discharge ratio of q^* = 0.250 is selected for validation in this study, as it generates a large separation zone and has a greater change in water-surface elevation. The ratio of the upstream main channel flow Q_m to the combined total flow Q_d is defined by q^*. All distances were normalized by the channel width, W, named as x^*, y^* and z^* for x/W , y/W and z/W respectively. The velocity components were normalized by the downstream average velocity, V_d , called u^* and v^* for u/V_d and v/V_d , respectively.

The simulation domain has been carefully chosen to represent the inflow and outflow boundaries. It is noted that the free-surface elevation is determined numerically and is not known before the computation. Therefore, the main channel length upstream of the branch channel is lengthened to 12W=10.97 m and the branch channel length is prolonged to 10W=9.14 m, so that the fully developed

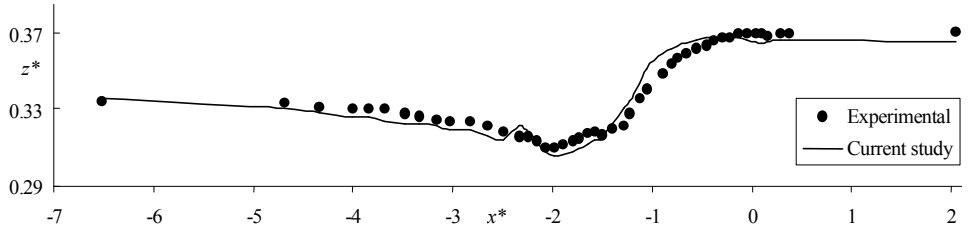

Fig. 10: Comparison of water surface elevation profiles

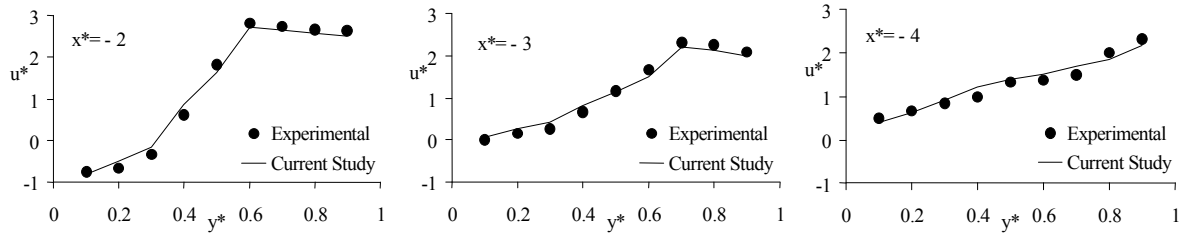

Fig. 11: Comparison of velocity profiles with experimental data

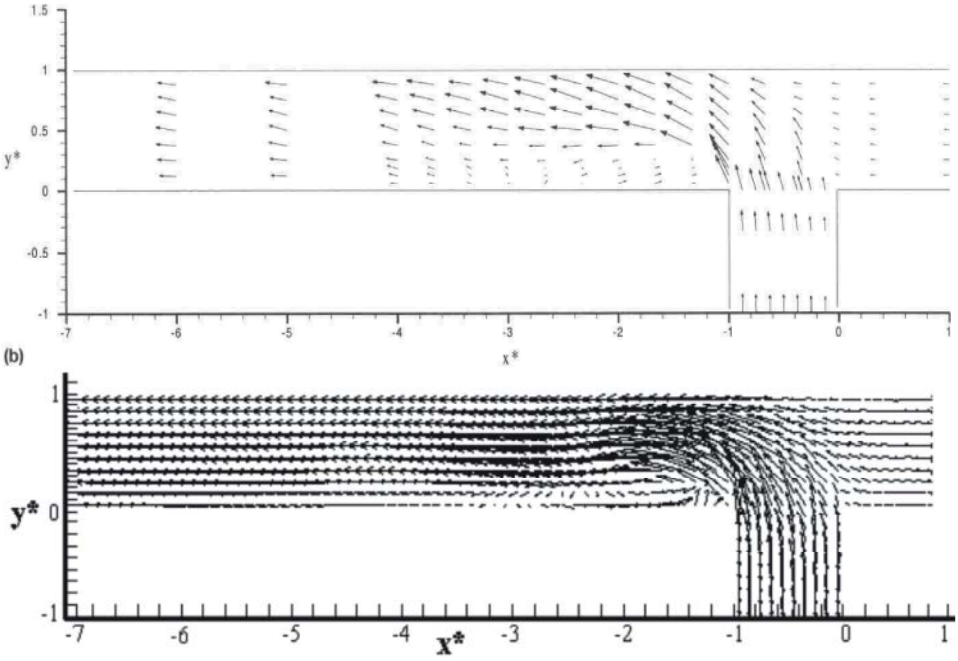

Fig. 12: Velocity pattern near the channel junction (a) measured data [33] (b) numerical predictions

flows are obtained near the downstream of the inlet boundaries. The length of main channel downstream of the branch channel is determined with 10*W*, where the flow depth is nearly constant (Fig. 9).

To simulate the flow, main channel has been introduced to the model as channel number 1 and the branch channel as channel number 2. Discharge value of 0.0425 and 0.1275 (m^3/s) has been applied at the u p stream boundary of main and branch channel respectively. Water depth of 0.296 m has been applied at the downstream boundary. Variation of water surface profile resulted from laboratory test and result of numerical modeling on main channel center line (at $y^* = 0.5$) is shown in Fig. 10. Also, velocity profile obtained from laboratory and numerical models is shown in Fig. 11.

Fig. 12 shows that the vortex length created after the branch channel in the laboratory model is twice the channel width. The vortex length in the presented research is 1.95 times the channel width. Comparison of the results shows the acceptable function of the used technique.

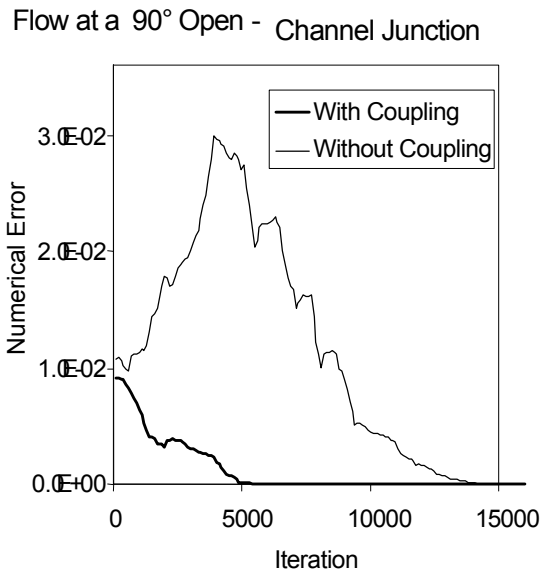

Fig. 13: Numerical error history at flow in 90° open-channel junction

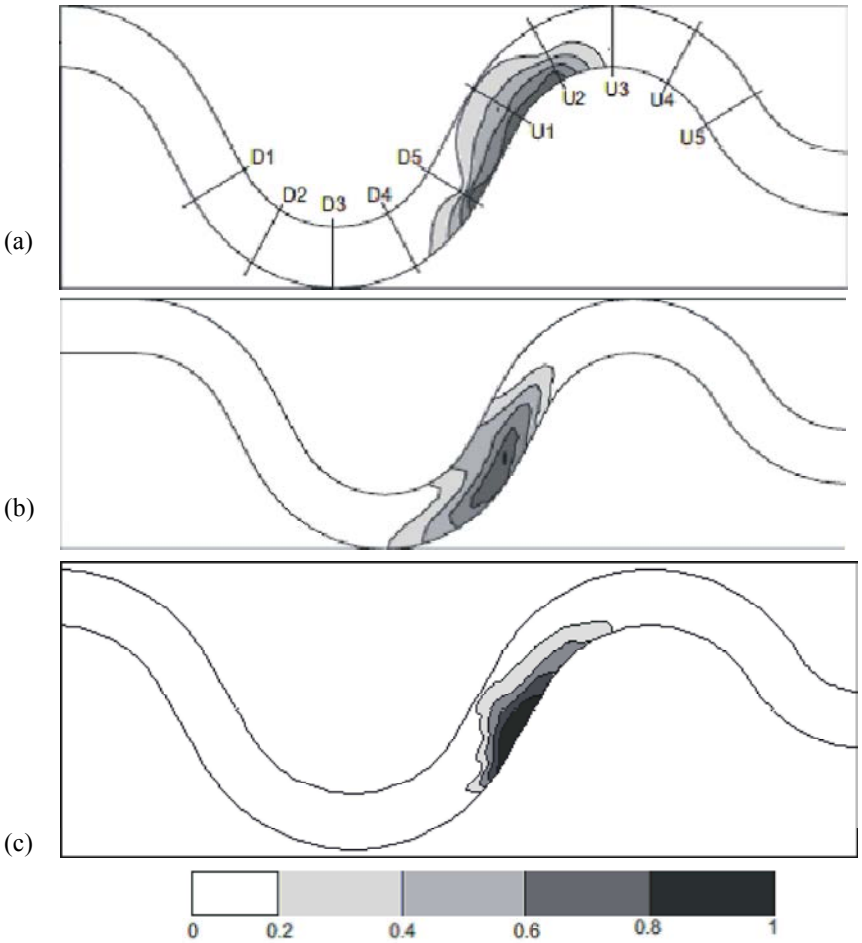

Fig. 14: Concentration contour at t =20s: (a) experimental result [34]; (b) numerical simulation by Lee and Seo [41]; (c) current study.

Convergence test has been carried out on the basis of numerical error history. As shown in Fig. 13, the coupled model has converged with fewer iterations and the effect of the used coupled model on the convergence of this test has been more than those of the other tests. Considering the same initial conditions, mere 2D model converged with more iteration than coupled 1D-2D model. Discharge in the branch channel is three times of the discharge in the main channel. Hence, the flow of the branch channel tends towards the main channel upstream during solution steps. However, when the effect of the main channel upstream boundary conditions dominates, the flow acquired its real form. This process was the cause the delay in the convergence of the mere 2D model. The coupled model did not experience such a problem and converged more rapidly.

Tracer Test in the S-curved Channel: To verify the developed environmental model, the data obtained by Baek *et al.* [34] from a tracer test in the laboratory meandering channel (Figure 14(a)) and the numerical results provided by Lee and Seo [41] (Figure 14(b)) are applied. Both figures present the contour distribution of non-dimensional concentration C/C_p for t=20s after the injection, where C_p is the peak concentration value at the concerned time. The S-curved laboratory channel is 15 m long, 1 m wide and 0.6 m deep. Among the various experimental cases in the Baek *et al.* case 101 was selected. This case was done under the condition of water depth of 0.1 m and flow rate of 0.03 m^3/s. Salt solution, maintained neutrally buoyant by adding alcohol, was used as a tracer. The initial concentration of instantaneously injected tracer was 100,000 mg/l and injection was treated as a vertical line source with a cylindrical injection equipment of 9.0 cm diameter.

The input hydrodynamic data, velocity and depth fields, for environmental model was obtained from the proposed hydrodynamic model. For cross sectional dispersion coefficient, Fischer *et al.* [42] proposed $D_T = 0.6HU_*$ in meandering channels. Also Elder [43] proposed $D_L = 5.93\ HU_*$ for longitudinal dispersion coefficient under the assumption of uniform flow with a logarithmic velocity profile along the vertical direction in an infinitely wide open channel.

To compare numerical results of current study with other previous data, computed non-dimensional concentrations after 20 s from the injection are illustrated in Figure 14(c). It can be seen that both computed tracer clouds follow the route of measured cloud and move along the right side of the channel where maximum velocity occurs. Furthermore, the shapes of both computed tracer clouds are almost similar to the measured cloud in terms of the longitudinal and transversal lengths of the clouds. Hence, it can be claimed that the presented numerical model can adequately explain the movement of tracer in the meandering channel.

DISCUSSION

Simple methods of discretization may have good results in simple geometries, but when there is discontinuity in the geometry, they may not work properly. To develop an accurate model to eliminate unexpected oscillations and non convergence in the results, special techniques can be used. Common schemes used to overcome such problems are artificial viscosity, T.V.D. McCormack, upwind, multi-grid, staggered mesh and so on [18-24].

It is worth mentioning that when the number of the elements involved in an equation discretization increases, the rate of convergence increases and oscillations in results decrease. For example, in discretization of advection term in 1D equation, using a third degree accuracy upwind scheme, there are four elements involved, but in a first degree accuracy upwind scheme there are only two elements involved. As another example, in the application of artificial viscosity method in 1D equation, an expression is added to the equation that causes more relation between depth and velocity parameters in three consecutive elements.

Since numerical errors and instability are low in 1D results, they can be used to moderate 2D results. In this paper, 2D flow parameters are linked with 1D flow variables in order to reduce 2D result oscillations and increase convergence.

It is supposed that the 1D flow parameter can be taken from a reliable 1D model and has acceptable accuracy, or it is gathered directly from the natural channel. It is known that 2D models usually give more information and details about flow behavior at different locations than 1D models do, but this does not mean that a 2D modeling is more precise. For example, it is possible that the discharge or water depth at a cross section in a 1D modeling is more precise than that of 2D modeling for the same channel.

Solving 2D flow equations, velocity components in both horizontal directions and the water surface elevation at each element is computed. Also, water surface elevation and the mean velocity at each cross section along a river can be found from 1D model.

In this paper 1D and 2D channel flow equations are solved simultaneously. This double solution can provide several advantages including: (a) finding 1D flow correction factor, β, for momentum equations to increase 1D model accuracy; (b) reducing numerical oscillation in 2D computations and increasing convergence; (c) increasing general computational speed due to oscillation reduction from double check scheme; (d) ability to analyze flow within narrow path and wide plain with both 1D and 2D models and (e) double check of results and increasing reliability of computations. It is to be mentioned that the proposed scheme is not a multigrid one because, in the multigrid solution, one set of equations is applied for different meshes but in this scheme two different sets of equations are applied.

CONCLUSIONS

Two dimensional shallow water flow equations are generally used to analyze flow pattern in wide rivers and open channels. A coupled 2D and 1D model is developed in this study to solve these equations. The 2D governing equations are discretized based on the finite volume method and solved by applying the ADI scheme. To reduce the numerical errors and divergence in the 2D analysis, the concept of applying 1D analysis results is presented and discussed in details.

Since there is almost ignorable numerical errors and instability in a 1D simulation, the results of 1D analysis can be applied as a general comparable solution against averages of 2D analysis results.

A 2D model is developed and modified, according to the mentioned point, that can compare and adjust 1D and 2D results. Momentum correction factor can be found from 2D model to apply in 1D simulation. Also averages of water level and discharges from elements across a section in 2D model can be compared with mean water level and section discharge in 1D simulation. These coupled models generate a hybrid simulation system that leads to some more reliable computational results.

Also, the new sequential technique has been applied to simulate a channel network. Each branch is discretized and the respected flow governing equations are solved separately. In the channel junction points, we need the adjacent branch data which are obtained from the prior step in the solution process and used in the calculation as the lateral discharge. This technique is used in 2D flow simulation of branching channels for the first time and can reduce coefficients matrix dimension; hence, the computational speed and the convergence rate are increased.

The hybrid model was applied to analyze three different case studies and flow results were compared with valid data. The comparison shows that the model can reliably predict flow parameters. The model converges rapidly and reduces the time and the volume of calculations to obtain the final results. Also, use was made of the results of flow modeling to develop the pollution transport model. The comparison of the results of the pollution and laboratory models shows the proper function of both hydraulic and pollution models. Although the model fits well to the laboratory test cases, it has to be tested for real long river flow.

REFERENCES

1. Mohamadian, A., D.Y. Le Roux, M. Tajrishi and K. Mazaheri, 2005. A mass conservative scheme for simulating shallow flows Over variable topographies using unstructured grid, Advances in Water Resources, 28: 523-539.
2. De Vriend, H., 1979. Flow measurements in a curved rectangular channel, Internal Rep. No. 9-79. Tech. Rep. Laboratory of Fluid Mechanics, Department of Civil Engineering, Delft University of Technology, Delft, The Netherlands,
3. Driver, D.M. and H.L. Seegmiller, 1985. Features of a reattaching turbulent shear layer in divergent channel flow, AIAA. J., 23: 163-171.
4. Molls, T. and M.H. Chaudhry, 1995. Depth-averaged open-channel flow model, Journal of Hydraulic Engineering, 121: 453-465.
5. Xiao-feng, Z. ,Z. Hong-wu and T. Takahashi, 2002. A new high order scheme for convection equation and its application, J. Hydrodynamics, 14: 81-86.
6. Capart, H., T.I. Eldho, S.Y. Huang, D.L. Young and Y. Zech, 2003. Treatment of natural geometry in finite volume river flow computations, Journal of Hydraulic Engineering, 129: 385-393.
7. Chanson, H., 2004. Environmental Hydraulics of Open Channel Flows, Australia: Butter Worth Heinemann,
8. Litrico, X. and V. Fromion, 2006. Boundary control of linearized Saint-Venant equations oscillating modes, Automatica, 42: 967-972.
9. Garcia, R. and R. Kahawitha, 1986. Numerical solution of the St. Venant equations with the Mac Cormack finite difference scheme, International J. Numerical Methods in Fluids, 6: 507-527.
10. Bellos, C., J. Soulis and J. Sakkas, 1991. Computation of two dimensional dam break induced flow, Advances in Water Res., 14: 31-41.

11. Fennema, R.J. and M.H Chaudhry, 1990. Explicit methods for 2D transient free-surface flows, Journal of Hydraulic Engineering, 116: 1013-1034.
12. Akanbi, A. and N. Katopodes, Model for flood propagation on initially dry land, Journal of Hydraulic Engineering, 114(1988): 689-706.
13. Zhao, D.H., H.W. Shen, G.Q. Tabios, J.S. Lai and W.Y. Tan, 1994. Finite-volume two dimensional unsteady-flow model for river basins, J. Hydraulic Engineering, 120: 863-883.
14. Abbasnia, A.H. and R. Ghiassi, Improvements on bed-shear stress formulation for pier scour computation, International Journal for numerical methods in fluids, Article first published online: 29 JUN (2010), DOI: 10.1002/fld.2372.
15. Yang, X.D., H.Y. Ma and Y.N Huang, 2005. Prediction of homogeneous shear flow and a backward-facing step flow with some linear and non-linear K-ε turbulence models, Communications in Nonlinear Science and numerical Simulation, 10 315-328.
16. Valiani, A., V. Caleffi and A. Zanni, 1999. Finite volume scheme for 2D shallow-water equations. Application to Malpasset dam break, Paper Presented at the 4th CADAM Meeting, November 18-19, Zaragoza, Spain,
17. Hirsch, C., 1990. Numerical computation of internal and external flows, Wiley J. and Sons, Chicester,
18. Alcrudo, F. and P.G Navarro, 1994. Computing two-dimensional flood propagation with a high resolution extension of McCormack's method, Paper presented at the International Conference on Modelling of Flooding Propagation over Initially Dry Areas, Milan, Italy,
19. Delis, A.J., C.P. Skeels and S.C. Ryrie, 2000. Implicit high - resolution methods for modelling one - dimensional open channel flow, Journal of Hydraulics Res., 38: 369-382.
20. Macchione, F. and M. Assunta Morelli, 2003. Practical aspects in comparing shock-capturing schemes for dam break problems, J. Hydraulic Engineering, 129: 187-195.
21. Mambretti, S., D. De Wrachien, E. Larcan, Debris flow and dam-breack flooding waves, 2008. Paper presented at the 36th International Symposium Actual Tasks on Agricultural Engineering, Opatija ,Croatia,
22. Zhao, D.H., H.W. Shen, J.S. Lai. and G.Q. Tabios, 1996. Approximate Riemann solvers in FVM for 2D hydraulic shock wave modeling, J. Hydraulic Engineering, 122: 692-702.
23. Zarrati, A.R. and Y.C. Jin, 2004. Development of a generalized multi-layer model for 3-D simulation of free surface flows', International Journal for Numerical Methods in Fluids, 46: 1049-1067.
24. Aliparast, M., 2009. Two-dimensional finite volume method for dam-break flow simulation, International J. Sediment Res., 24: 99-107.
25. Miglio, E., S. Perotto and F. Saleri, 2005. Model coupling techniques for free-surface flow problems: Part I, Nonlinear Analysis, 63: 1885-1896.
26. Fang-li, Y., Z. Xiao-feng. and T. Guang-ming, 2007. One and two-dimensional coupled hydrodynamics model for dam break flow, J. Hydrodynamics, 19: 769-775.
27. Gejadze, I.Y. and J. Monnier, 2007. On a 2D 'zoom' for the 1D shallow water model:Coupling and data assimilation, Computer Methods in Applied Mechanics and Engineering, 196: 4628-4643.
28. Wang, J., Y. He. and H. Ni, 2003. Two-dimensional free surface flow in branch channels by a finite-volume TVD scheme, Advances in Water Resources, 26: 623-633.
29. Yousefi, S., R. Ghiassi and Sa. Yousefi, 2010. Modelling and analyzing flow diversion in branching channels with symmetric geometry', River research and applications,Article first published online: DOI: 10.1002/rra.1393,
30. Neary, V.S. and F. Sotiropoulos, 1996. Numerical investigation of laminar flows through 90-degree diversions of rectangular cross-section, Computers and Fluids, 25: 95-118.
31. Huang, J., L.J. Weber and Y.G. Lai, 2002. Three-dimensional numerical study of flows in open-channel junctions, J. Hydraulic Engineering, 128: 268-280.
32. Patankar, S.V., 1980. Numerical Heat Transfer and Fluid Flow, Hemisphere Publishing Corporation, New York,
33. Weber, L.J., E.D. Schumate. and N. Mawer, 2001. Experimental at a 90° open-channel junction, Journal of Hydraulic Engineering, 127: 340-350.
34. Baek, K., I.W. Seo. and S.J. Jeong, 2006. Evaluation of dispersion coefficient in meandering channels from transient tracer tests, J. Hydraulic Engineering, 132: 1021-1032.
35. Fischer, H.B., 1973. 'Longitudinal Dispersion and Turbulent Mixing in Open-Channel Flow', Annual Review of Fluid Mechanics, 5: 59-78, Inc. Paolo Alto, Calif.,

36. Stoker, J.J., 1957. Water Waves, the Mathematical Theory with Applications, Interscience, New York,
37. Chung, T.J., 2002. Computational Fluid Dynamics, Cambridge University,
38. Ghiassi, R., Mathematics. and Computer Application in Nature Simulation. Lecture Notes. University of Tehran, 2004.
39. Manoochehri, A., 2008. One dimensional unsteady flow simulation in channel network, MSc thesis, Faculty of civil engineering, University of Tehran,
40. Tamai, N., K. Ikeuchi, A. Yamazaki and A.A. Mohamed, 1983. Experimental analysis on the open channel flow in rectangular continuous bends, J. Hydroscience and Hydraulic Engineering, 2: 17-31.
41. Lee, M.E. and I.W. Seo, 2007. Analysis of pollutant transport in the Han river with tidal current using a 2D finite element model, J. Hydro-Environmental Res., 1: 30-42.
42. Fischer, H.B., E.J. List, R.C.Y. Koh, J. Imberger. and N.H. Brooks, 1979. Mixing in inland and coastal waters, Academic, New York,
43. Elder, J.W., 1959. The dispersion of marked fluid in turbulent shear flow' J. Fluid Mechanics, 5: 544-560.